Dynamics of the crystal lattice of $RBa_2Cu_3O_{7-\delta}$: relationship between the vibrational spectra and anisotropy of the structure

M. F. Limonov

A. F. Ioffe Physicotechnical Institute, 194021 St. Petersburg, Russia

A. P. Mirgorodskiĭ

Institute of Silicate Chemistry, Russian Academy of Sciences, St. Petersburg, Russia

(Submitted 22 March 1994)
Zh. Eksp. Teor. Fiz. **106**, 1794–1813 (December 1994)

A model of the potential function of the crystal lattices of $RBa_2Cu_3O_{7-\delta}$ (the so-called '123' structure) is proposed using the valence-force-field approximation. The results of calculating the dynamic properties of the lattices of 123 compounds, including detailed information on the optical vibrations and dispersion of the phonon branches in the Brillouin zone, the dependence of the frequencies on the composition, the macroscopic elastic characteristics, and the microscopic behavior of the structure under hydrostatic compression, are presented. The vibrational spectra of isolated layers forming a 123 crystal structure are analyzed in the model approximation. The similarity of the "wave-like" restructuring of 123 compounds observed when their composition is varied and under hydrostatic compression is noted. The corresponding concentration dependence of the frequencies and the baric dependence of the interatomic distances are described with consideration of the dynamic interaction of the CuO_2 layers through Y atoms. It is shown that the optical vibrations can be divided into interlayer and intralayer vibrations. It is concluded that the phonon subsystem in layered perovskite-like superconductors exhibits quasi-two-dimensional behavior. © *1994 American Institute of Physics.*

1. INTRODUCTION

The dynamics of the crystal lattice of the perovskite-like compounds $RBa_2Cu_3O_{7-\delta}$ (the so-called 123 compounds) have attracted great attention in connection with the discussion of the role of phonons in the carrier pairing mechanism in high-T_c superconductors. In fact, there are indications of the existence of a strong electron–phonon interaction in these compounds, and it has been established experimentally that the transition to the superconducting state is accompanied by several unusual features in the behavior of the vibrational subsystem.[1–4] This has been responsible for the unwavering interest in theoretical and experimental investigations of the dynamic properties of perovskite-like superconductors. Pertinent calculations have been performed for the 123 system in various models (see, for example, Refs. 5–10, as well as the reviews in Refs. 4 and 11). Together with the data from a group-theoretical analysis, their results made it possible to reliably interpret the Raman spectra, as well as the infrared (IR) reflection and absorption spectra.

Nevertheless, there are several questions, whose solution may promote our understanding of the role of the phonon subsystem in the superconductivity mechanism, but which still remain open.

In particular, the crystal lattices of perovskite-like superconductors, including $YBa_2Cu_3O_7$, have a clearly expressed anisotropic layered structure, which is responsible for some specific properties, for example, the repeatedly discussed quasi-two-dimensional behavior of the electronic subsystem (see, for example, Ref. 12). However, attention has not yet been focused on the influence of this anisotropy on the vibrational subsystem. The main concern of this paper is to fill in this gap.

The model of the potential function of several stoichiometric 123 compounds proposed in the present work was used to obtain and analyze information on their dynamic properties, including detailed data on the vibrations at the center of the Brillouin zone, the dispersion of the phonon branches throughout the Brillouin zone, the dependence of the frequencies on the composition, and the macroscopic characteristics, as well as data on the microscopic behavior of the structure under hydrostatic compression. As a result it was concluded that the phonon subsystem in a 123 crystal lattice exhibits quasi-two-dimensional behavior, which, in our opinion, is a common feature of perovskite-like superconductors.

Consideration of the quasi-two-dimensional behavior is a necessary condition for describing the electron-phonon interaction in these compounds, and if phonons participate in carrier pairing, it would be a necessary condition for describing the actual mechanisms of high-T_c superconductivity.

Special attention has been focused on the "wave-like" restructuring of 123 compounds, which is observed both when their composition is varied and under hydrostatic compression. The results of our own experimental investigations of the Raman spectra of various 123 compounds[13–18] and published data (see, for example, Refs. 4 and 19) were used in the calculations.

 1063-7761/94/120973-12$10.00

2. CALCULATION SCHEME AND FORCE FIELD MODEL OF THE CRYSTAL LATTICE OF 123 COMPOUNDS

We briefly describe the formalism which was used in the calculations discussed in this paper.

It is convenient to consider the relationship between the vibrational motions of atoms and the macroscopic strain of a lattice, i.e., between its internal microscopic and external macroscopic degrees of freedom, in terms of the following expression for the density of the internal energy W of the strained crystal, which is described in a mixed basis of the initial (nonequilibrium) uniform strains U_i and the internal degrees of freedom Q_λ, i.e., normal coordinates at the center of the Brillouin zone:[20]

$$W=\frac{1}{2}U_iC^0_{ik}U_k+\frac{1}{2}Q_\lambda\nu^2_\lambda Q_\lambda+Q_\lambda F_{\lambda k}U_k \tag{1}$$

(here and in the following summation is implied over repeated indices). The coefficients C^0_{ik}, ν_λ, and $F_{\lambda k}$ are the "external" component of the elastic constant, the frequency of the phonon at the center of the Brillouin zone, and the optoacoustic coupling parameter.

The condition for a stationary state $\partial W/\partial Q_\lambda=0$ leads to the relation

$$\nu^2_\lambda Q_\lambda=-F_{\lambda k}U_k, \tag{2}$$

which makes it possible to eliminate Q_λ from (1) and to obtain the following expression for the elastic constants of the crystal:

$$C_{ik}=C^0_{ik}-\frac{F_{\lambda i}F_{\lambda k}}{\nu^2_\lambda}. \tag{3}$$

In a basis of the microscopic natural coordinates q_m describing the variations of the relative positions of the atoms (i.e., interatomic distances, angles between bonds, etc.), W has the form

$$W=\frac{1}{2}q_mK_{mn}q_n, \tag{4}$$

where K_{mn} denotes the force constants, which are adjustable parameters of the model in our case.

Since C^0_{ik}, ν^2_λ, and $F_{\lambda k}$ are formally second partial derivatives of W with respect to U_i and Q_λ, they can be obtained from (4) in the following forms:

$$C^0_{ik}=\frac{\partial q_m}{\partial U_i}K_{mn}\frac{\partial q_n}{\partial U_k}, \tag{5}$$

$$\nu^2_\lambda=\frac{\partial q_m}{\partial Q_\lambda}K_{mn}\frac{\partial q_n}{\partial Q_\lambda}, \tag{6}$$

$$F_{\lambda k}=\frac{\partial q_m}{\partial Q_\lambda}K_{mn}\frac{\partial q_n}{\partial U_k}, \tag{7}$$

where $\partial q_n/\partial U_k$ and $\partial q_m/\partial Q_\lambda$ are the vectors of the external uniform strains and the normal coordinates at the center of the Brillouin zone, respectively. The former are found directly from the geometry of the lattice, and the latter are found by diagonalizing the matrix K_{mn} and normalizing its eigenvectors. The relationship between the basis of the Cartesian atomic displacements x and the coordinates q, $q=Bx$, permits consideration of the vibrational problem in both bases.

The vector of the total (i.e., compensated) uniform strain is defined as the complete derivative

$$\frac{dq_m}{dU_i}=\frac{\partial q_m}{\partial U_i}+\frac{\partial q_m}{\partial Q_\lambda}\frac{\partial Q_\lambda}{\partial U_i},$$

which may be written with consideration of expression (2) in the form

$$\frac{dq_m}{dU_i}=\frac{\partial q_m}{\partial U_i}-\frac{\partial q_m}{\partial Q_\lambda}\frac{F_{\lambda i}}{\nu^2_\lambda}. \tag{8}$$

Knowledge of the values of dq_m/dU_i is sufficient for determining the picture of internal microscopic strains resulting from any macroscopic uniform distortions of the lattice, including those appearing under hydrostatic compression.

The foregoing formalism was used in the present work in calculations performed by the CRYME (CRYstal MEchanics) package.[21] The potential functions of the 123 crystals considered were similarly described in the approximation of a short-range valence force field of general form. This approach was previously employed successfully in modeling the dynamic properties of complex oxides with an ionic-covalent type of chemical bonding.[22,23] We note that compounds of this type underlie the synthesis of various perovskite-like superconductors.

The crystal structure of $RBa_2Cu_3O_{7-\delta}$ is well known. The structural data were borrowed from Ref. 24 for $YBa_2Cu_3O_{7-\delta}$ and from Ref. 25 for $GdBa_2Cu_3O_7$ (Table I). In this paper we use the notation for the atoms introduced in Refs. 4 and 19: an oxygen atom belonging to a definite metal–oxygen layer is designated as O with a subscript indicating the respective metal atom (Fig. 1a).

The original basis of natural vibrational coordinates included the interatomic interactions over distances less than 3.6 Å and the O–Cu–O angles. The corresponding force field consisted of the constants S_i, which describe the diagonal two-center interactions, the constants B_i, which describe the diagonal three-center interactions (i.e., the elasticities of the O–Cu–O angles), and the off-diagonal constants H_i, which determine the dynamic interaction of two bonds sharing a common atom.

The values of the force constants were determined by adjusting the theoretical values of the frequencies of the vibrations at the center of the Brillouin zone to the corresponding experimental values, including the frequencies of the Raman-active vibrations of $YBa_2Cu_3O_7$ (Ref. 26), $YBa_2Cu_3O_6$ (Ref. 27), and $GdBa_2Cu_3O_7$ (Refs. 16 and 18) crystals and the IR-active vibrations of $YBa_2Cu_3O_{6.8}$ (Ref. 28) and $YBa_2Cu_3O_6$ (Ref. 29). The experimental values are presented in Tables II and III, and the sets of force constants obtained as a result of such a procedure are presented in Table I.

We note that these compounds are characterized by the presence of a large number of Cu–O bonds of various length (Table I). It is seen from Fig. 2 that the values of the corresponding S_i obtained by the method indicated above for three compounds fit one common curve, giving the empirical

TABLE I. Force constants and structural parameters[a] for $YBa_2Cu_3O_7$ (for a three-dimensional lattice and for calculations in the isolated layer approximation), as well as for $YBa_2Cu_3O_6$ and $GdBa_2Cu_3O_7$ crystals.

Force constants	Atoms determining interaction	$YBa_2Cu_3O_7$			$YBa_2Cu_3O_6$		$GdBa_2Cu_3O_7$	
		Length or angle	Constants		length or angle	Const.	length or angle	Const.
			Cryst.	Layers				
S_1	$Cu1-O_{Ba}$	1.837	1.8	0	1.822	1.9	1.918	1.5
S_2	$Cu-O_{Cu}$	1.931	1.35	1.35	1.944	1.3	1.940	1.3
S_3	$Cu1-O_{Cu1}$	1.943	1.3	1.3	-	-	1.948	1.27
S_4	$Cu-O'_{Cu}$	1.961	1.25	1.25	1.944	1.3	1.957	1.25
S_5	$Cu-O_{Ba}$	2.315	0.7	0	2.411	0.4	2.211	0.9
S_6	$O'_{Cu}-R$[b]	2.384	0.55	0	2.395	0.55	2.456	0.45
	$O_{Cu}-R$	2.400	0.55	0	2.395	0.55	2.422	0.45
S_7	$Ba-O_{Ba}$	2.743	0.27	0.27	2.763	0.25	2.744	0.27
S_8	$Ba-O_{Cu1}$	2.880	0.23	0	-	-	2.875	0.23
S_9	$Ba-O'_{Cu}$	2.960	0.2	0	2.937	0.22	2.902	0.22
S_{10}	$Ba-O_{Cu}$	2.996	0.2	0	2.937	0.22	2.991	0.2
S_{11}	$O_{Cu}-O_{Cu}$	2.817	0.2	0	2.840	0.22	2.877	0.2
	$O'_{Cu}-O'_{Cu}$	2.854	0.2	0	2.840	0.22	3.064	0.2
S_{12}	Ba–Cu1	3.474	0.2	0	3.544	0.2	3.473	0.2
S_{13}	R–Cu	3.207	0.1	0	3.196	0.1	3.231	0.1
B_1	$O_{Cu}-Cu-O'_{Cu}$	88.9	0.45	0.45	89.1	0.45	89.2	0.45
B_2	$O_{Ba}-Cu1-O_{Cu1}$	90.0	0.45	0	-	-	90.0	0.45
B_3	$O_{Ba}-Cu-O'_{Cu}$	97.7	0.15	0	97.2	0.2	95.5	0.15
	$O_{Ba}-Cu-O_{Cu}$	98.4	0.15	0	97.2	0.2	98.3	0.15
H_1	$O_{Ba}-Cu1/Cu1-O_{Ba}$	-	−0.2	0	-	−0.3	-	−0.05
H_2	$O_{Cu}-R/R-O_{Cu}$	-	0.13	0	-	0.14	-	0.13

[a]The force constants are given in the following units: S_i, mdyne/Å; B_i, mydne·Å; H_i, mdyne/Å. The distances are given in angstroms, and the angles in degrees

[b]R=Y or Gd.

dependence of S(Cu–O) on the interatomic distance in the 1.8–2.4 Å range. Thus, this set of values of S_i is internally self-consistent in a certain sense [this also applies to other sets of constants, for example, S(Ba–O)], and the effective number of independent parameters is smaller than the number given in Table I. In this case a significantly larger number of experimental data are adequately described, which should be a necessary condition for any phenomenological model claiming to be physically plausible.

3. DYNAMICS OF THE CRYSTAL LATTICE OF 123 COMPOUNDS

The unit cells of $YBa_2Cu_3O_7$ (D^1_{2h}) and $YBa_2Cu_3O_6$ (D^1_{4h}) crystals each contain one formula unit. At the center of the Brillouin zone the fundamental vibrations are distributed among the irreducible representations in the following manner:

$$\Gamma(D^1_{2h})=5A_g+5B_{2g}+5B_{3g}+8B_{1u}+8B_{2u}+8B_{3u}$$

$$\Gamma(D^1_{4h})=4A_{1g}+B_{1g}+5E_g+6A_{2u}+B_{2u}+7E_u, \qquad (9)$$

where the $B_{1u}+B_{2u}+B_{3u}$ modes (D^1_{2h}) and the $A_{2u}+E_u$ modes (D^1_{4h}) are acoustic.

Since both crystal structures have a symmetry center, the fundamental optical vibrations satisfy alternative selection rules: the even (g) vibrations can be active only in the Raman spectra, and the odd (u) vibrations can be active only in the IR spectra.

In a $D^1_{2h}\leftrightarrow D^1_{4h}$ phase transition (which occurs at the intermediate values $\delta\approx 0.6$ as a result of redistribution of the oxygen atoms in the $Cu1O_{Cu1}$ plane), the vibrations of the orthorhombic and tetragonal lattices correlate in the following manner: $5A_g\leftrightarrow 4A_{1g}+B_{1g}$, $5B_{2g}+5B_{3g}\leftrightarrow 5E_g$, $7B_{1u}\leftrightarrow 6A_{2u}+B_{2u}$, $7B_{2u}+7B_{3u}\leftrightarrow 7E_u$.

Table II presents the calculated values of the optical vibration frequencies of $YBa_2Cu_3O_7$ at three points in the Brillouin zone: Γ(0,0,0), Z(0,0,1/2), and Y(0,1/2,0). The table also gives the relative amplitudes of the atomic displacements determining the forms of the long-wavelength optical vibrations. The results of the calculations for the structure of $YBa_2Cu_3O_6$ are given in Table IV.

The calculated dispersion branches of the $YBa_2Cu_3O_7$ lattice along the $(0,0,\zeta)$ and $(0,\zeta,0)$ directions of the Brillouin zone are presented in Fig. 3.

Figure 5 presents the experimental and calculated values of the frequencies of the vibrations of the oxygen atoms along the z axis in various compounds with the 123 structure. In the case of $GdBa_2Cu_3O_7$ the experimental data are confined to the frequencies of vibrations of type A_g; therefore, for the sake of brevity, we shall not present all the calculated

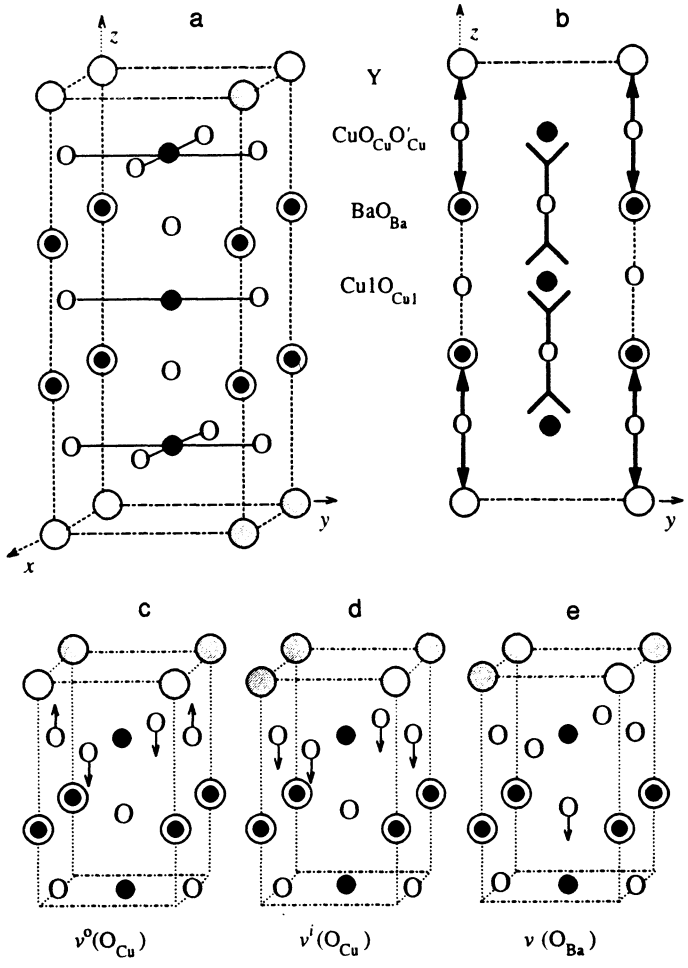

FIG. 1. a) Crystal structure of $YBa_2Cu_3O_7$. b) Diagram of the variations of the bond lengths when the oxygen content is varied on the Y atoms are replaced with atoms of rare-earth elements[24,25,38] in the $YBa_2Cu_3O_7$ lattice projected onto the yz plane. Here $\leftrightarrow$ indicates an increase in the bond length, and $>\!-\!<$ indicates a decrease. c–f) Displacement vectors corresponding to three high-frequency A_g modes.

results obtained for this compound, especially since the characteristic changes in the vibrational subsystem resulting from the Y→Gd substitution are clearly seen in the example of the phonons of A_g symmetry.

Good correspondence between the calculated frequencies at the center of the Brillouin zone and the experimental data was generally obtained (Tables II and III). We also note that the frequencies for $\mathbf{k}\neq 0$ were not included in the adjustment procedure; nevertheless, the calculated dispersion curves satisfactorily describe the experimental plots (Fig. 3). Some differences between the theoretical and experimental course of the dispersion curves (for example, the fact that the branches with frequencies ≈ 600 cm^{-1} exhibit slight dispersion in the Γ→Y direction, while the branches obtained in the calculation had no dispersion) point out deficiencies in the description of the potential function of the lattice, which should be attributed primarily to the lack of explicit consideration of the electrostatic forces and the small number of off-diagonal force constants.

Let us discuss the modes of vibration of the $YBa_2Cu_3O_7$ crystal lattice presented in Table II. The conclusions which will be drawn here are also valid to a considerable extent for $YBa_2Cu_3O_6$ and $GdBa_2Cu_3O_7$.

When the vibrational spectra of perovskite-like superconductors are interpreted, the high-frequency modes are customarily associated with vibrations of the oxygen atoms, and the low-frequency modes are associated with vibrations of the heavy atoms. It is then assumed that each vibration is determined predominantly by atoms of one kind (see, for example, Ref. 30). However, according to the results of our calculations, another description of the optical vibrations, which we shall propose below, is more suitable.

We recall that compounds with the 123 structure have a clearly expressed layered structure. In our model of the potential function, this feature was not specified *a priori* in any way by the choice of parameters or by their estimated numerical values. Nevertheless, an analysis of the results obtained objectively reveals that the optical vibrations should be divided into intralayer and interlayer vibrations.

Let us first consider the low-frequency optical modes. As is seen from Tables II and III, most such vibrations correspond to displacements of atoms in different layers relative to one another. In some cases the amplitudes of the displacement of atoms belonging to the same layer are close, i.e., each layer is displaced as a single unit. Such vibrations may be regarded as interlayer vibrations, since the elastic forces determining them are associated mainly with interlayer interactions.

A clear-cut example of interlayer vibrations is provided by pairs of low-frequency modes of B_{2g} and B_{3g} symmetry (Table II). The vibrations at 78 and 79 cm^{-1} correspond to the in-phase displacement of BaO_{Ba} and $CuO_{Cu}O'_{Cu}$ layers in the basal plane relative to the stationary Y and $CuIO_{CuI}$ lay-

TABLE II. Calculated values of the frequencies (cm^{-1}) at the points $\Gamma(0,0,0)$, $Z(0,0,1/2)$, and $Y(0,1/2,0)$ in the Brillouin zone and components of the atomic displacements at the point Γ in the Brillouin zone for the crystal structure of $YBa_2Cu_3O_7$, as well as results of the calculation of the frequencies within noninteracting layers.

Experiment[a] (Ref. 26)	Calculation: Crystal Γ	Z	Y	Layers	Atomic displacement at the point Γ in the Brillouin zone[b]
					A_g
117	110	74	123	0	$6^z Ba + (1^z Cu + 1^z O_{Cu} + 1^z O'_{Cu})$
148	151	164	164	0	$3^z O_{Ba} + (9^z Cu + 1^z O_{Cu} + 1^z O'_{Cu})$
335	335	335	343	73	$13^z O_{Cu} - 12^z O'_{Cu}$
438	439	439	496	106	$12^z O_{Cu} + 13^z O'_{Cu} - 1^z Cu - 1^z O_{Ba}$
502	502	502	501	41	$17^z O_{Ba} - 1^z Cu$
					B_{2g}
-	78	90	116	0	$(5^z Ba + 5^z O_{Ba}) + (4^z Cu + 4^z O_{Cu} + 2^z O'_{Cu})$
-	103	99	117	0	$(3^z Ba + 2^z O_{Ba}) - (7^z Cu + 7^z O_{Cu} + 3^z O'_{Cu})$
210	261	261	248	249	$17^z O_{Ba} - 2^z Ba - 1^z O'_{Cu}$
330	357	357	352	241	$17^z O'_{Cu} - 1^z Cu - 2^z O_{Cu}$
575	596	596	596	594	$16^z O_{Cu} - 4^z Cu + 1^z O'_{Cu}$
					B_{3g}
-	79	89	95	0	$(5^y Ba + 4^y O_{Ba}) + (3^y Cu + 2^y O_{Cu} + 3^y O'_{Cu})$
-	104	101	113	0	$(2^y Ba + 1^y O_{Ba}) - (7^y Cu + 3^y O_{Cu} + 7^y O'_{Cu})$
303	310	310	290	253	$17^y O_{Ba} - 1^y Ba - 1^y O_{Cu}$
330	361	361	382	245	$17^y O_{Cu} - 1^y Cu + 1^y O_{Ba} - 2^y O'_{Cu}$
575	575	575	512	573	$16^y O'_{Cu} - 4^y Cu + 1^y O_{Cu}$

Experiment[a] (Ref. 28)	Calculation: Crystal Γ	Z	Y	Layers	Atomic displacement at the point Γ in the Brillouin zone[b]
					B_{1u}
113	121	124	120	0	$6^z Y-(4^z Ba-1^z O_{Ba})-2^z O_{Cu1}+(4^z Cu+2^z O_{Cu}+2^z O'_{Cu})$
154	139	129	237	0	$7^z Y+(1^z Ba-5^z O_{Ba})+(5^z Cu1+2^z O_{Cu1})+(5^z Cu-3^z O_{Cu}-3^z O'_{Cu})$
191	227	228	239	0	$2^z Y-(1^z Ba-6^z O_{Ba})+(8^z Cu1+7^z O_{Cu1})-(5^z Cu+2^z O_{Cu}+1^z O'_{Cu})$
281	264	264	265	73	$13^z O_{Cu}-12^z O'_{Cu}$
311	295	294	270	106	$11^z O_{Cu}+11^z O'_{Cu}-4^z Y-1^z Ba+1^z Cu1-2^z Cu+1^z O_{Ba}$
565	336	336	372	0	$24^z O_{Cu1}-1^z Ba-3^z Cu1+1^z Cu-3^z O_{Ba}$
610	620	620	619	41	$15^z O_{Ba}-7^z Cu1-1^z Cu+1^z O_{Cu1}$
					B_{3u}
-	64	38	114	0	$5^z Y-(3^z Ba+3^z O_{Ba})-(4^z Cu1+3^z O_{Cu1})+(5^z Cu+5^z O_{Cu}+4^z O'_{Cu})$
-	126	126	117	0	$(2^z Ba+3^z O_{Ba})-(11^z Cu1-4^z O_{Cu1})-(1^z Cu+1^z O_{Cu})$
181	153	153	125	0	$8^z Y-(5^z Cu+5^z O_{Cu}-2^z O'_{Cu})-1^z Ba$
240	212	212	215	0	$24^z O_{Cu1}-1^z Ba-4^z O_{Ba}$
345	262	262	248	249	$16^z O_{Ba}-2^z Ba-1^z O'_{Cu}+4^z O_{Cu1}$
477	371	371	367	241	$17^z O'_{Cu}-3^z Y-1^z Cu-2^z O_{Cu}$
590	596	596	596	594	$16^z O_{Cu}-4^z Cu+1^z O'_{Cu}$
					B_{2u}
-	65	40	104	0	$5^y Y-(3^y Ba+3^y O_{Ba})-(4^y Cu1+4^y O_{Cu1})+(5^y Cu+4^y O_{Cu}+5^y O'_{Cu})$
-	153	154	270	0	$4^y Y+(3^y Ba-1^y O_{Ba})-(8^y Cu1+8^y O_{Cu1})-(3^y Cu-2^y O_{Cu}+3^y O'_{Cu})$
-	156	155	283	0	$7^y Y-2^y Ba+(5^y Cu1+6^y O_{Cu1})-(4^y Cu-2^y O_{Cu}+4^y O'_{Cu})$
-	315	315	331	253	$17^y O_{Ba}-1^y Ba-2^y Cu1-1^y O_{Cu}-3^y O_{Cu1}$
-	375	375	348	245	$17^y O_{Cu}-3^y Y+1^y Cu-2^y O'_{Cu}$
-	575	575	512	573	$16^y O'_{Cu}-4^y Cu+1^y O_{Cu}$
-	593	593	525	588	$22^y O_{Cu1}-6^y Cu1+1^y O_{Ba}$

[a]Experimental data from the Raman spectra of $YBa_2Cu_3O_7$ (Ref. 26) and the IR spectra of $YBa_2Cu_3O_{6.8}$ (Ref. 28) are presented. The IR spectra were investigated under $E \perp z$ polarization without separation into B_{2u} and B_{3u} components. The experimental data were assigned to B_{3u} symmetry on a pure conditional basis.

[b]Amplitudes of the atomic displacements rounded to integer values are presented. Atomic displacements with amplitudes less than 0.5 are not indicated. The displacements of atoms belonging to the upper half of the unit cell are given. The mirror-image atoms in the lower half are displaced in phase with them in the case of odd vibrations and in antiphase in the case of even vibrations.

TABLE III. Calculated and experimental values of the frequencies (cm^{-1}) and calculated components of the atomic displacements[a] at the center of the Brillouin zone for $YBa_2Cu_3O_6$.

Experiment[27]		Calculation	Experiment[29]		Calculation
		A_{1g}			A_{2u}
110	98	$6^z Ba + (1^z Cu + 1^z O_{Cu} + 1^z O'_{Cu})$	108	116	$5^z Y - (4^z Ba - 1^z O_{Ba}) + (5^z Cu + 2^z O_{Cu} + 2^z O'_{Cu})$
144	138	$(-1^z Ba + 2^z O_{Ba}) + (9^z Cu + 1^z O_{Cu} + 1^z O'_{Cu})$	156	137	$7^z Y + (1^z Ba - 6^z O_{Ba}) - 6^z Cu1 - (4^z Cu - 3^z O_{Cu} - 3^z O'_{Cu})$
			216	193	$3^z Y - (1^z Ba - 7^z O_{Ba}) + 8^z Cu1 - (5^z Cu + 1^z O_{Cu} + 1^z O'_{Cu})$
456	454	$12^z O_{Cu} + 12^z O'_{Cu} - 2^z O_{Ba}$	370	298	$11^z O_{Cu} + 11^z O'_{Cu} - 4^z Y - 1^z Ba + 1^z Cu1 - 1^z Cu$
475	466	$17^z O_{Ba} - 1^z Cu + 1^z O_{Cu} + 1^z O'_{Cu}$	640	623	$15^z O_{Ba} - 7^z Cu1$
		B_{1g}			B_{2u}
343	345	$13^z O_{Cu} - 13^z O'_{Cu}$	-	269	$13^z O_{Cu} - 13^z O'_{Cu}$
		E_g^b			E_u^b
-	66	$(5^z Ba + 5^z O_{Ba}) + (3^z Cu + 3^z O_{Cu} + 2^z O'_{Cu})$	69	69	$5^z Y - (3^z Ba + 2^z O_{Ba}) - 5^z Cu1 + (5^z Cu + 5^z O_{Cu} + 3^z O'_{Cu})$
-	105	$(2^z Ba + 1^z O_{Ba}) - (7^z Cu + 8^z O_{Cu} + 3^z O'_{Cu})$	120	126	$1^z Y - (3^z Ba + 3^z O_{Ba}) + 11^z Cu1 + (1^z Cu + 1^z O_{Cu})$
			189	154	$8^z Y - (5^z Cu + 5^z O_{Cu} - 2^z O'_{Cu}) - 1^z O_{Ba}$
-	255	$17^z O_{Ba} - 2^z Ba - 1^z O'_{Cu}$	248	255	$17^z O_{Ba} - 2^z Ba - 1^z O'_{Cu} - 1^z O_{Cu1}$
-	361	$17^z O'_{Cu} - 1^z Cu - 2^z O_{Cu}$	355	374	$17^z O'_{Cu} - 3^z Y - 1^z Cu - 2^z O_{Cu}$
-	587	$16^z O_{Cu} - 4^z Cu + 1^z O'_{Cu}$	579	587	$16^z O_{Cu} - 4^z Cu + 1^z O'_{Cu}$

[a]Amplitudes of the atomic displacements rounded to integer values are presented. Atomic displacements with amplitudes less than 0.5 are not indicated. The displacements of atoms belonging to the upper half of the unit cell are given. The mirror-image atoms in the lower half are displaced in phase with them in the case of odd vibrations and in antiphase in the case of even vibrations.

[b]The x components of the atomic displacements are given.

ers, and the vibrations at 103 and 104 cm^{-1} correspond to antiphase displacement. The low-frequency vibrations of B_{2u} and B_{3u} symmetry have similar forms. For example, the B_{3u} frequency at 64 cm^{-1} corresponds to the antiphase displacement of Y and $CuO_{Cu}O'_{Cu}$ layers relative to BaO_{Ba} and $Cu1O_{Cu1}$ layers.

The interlayer character of the low-frequency vibrations of A_g and B_{1u} symmetry is not so clearly expressed, although layers displaced relative to one another can be identified in these cases too.

The high-frequency vibrations have an entirely different nature. Most of them are determined by the displacement of oxygen atoms belonging to the same layer. The amplitudes of the displacements of the remaining atoms are approximately an order of magnitude smaller. Therefore, such vibrations may be regarded as intralayer vibrations.

As an example, we cite three intralayer modes of A_g symmetry. The 335 cm^{-1} mode corresponds to antiphase vibrations of oxygen atoms belonging to a $CuO_{Cu}O'_{Cu}$ layer parallel to the z axis, and the 439 cm^{-1} mode corresponds to the analogous synphase vibrations. The 502 cm^{-1} mode is determined by the displacement of the oxygen atoms of a BaO_{Ba} layer along the z axis (Table II and Fig. 1). These vibrations are designated as $\nu^o(O_{Cu})$, $\nu^i(O_{Cu})$, and $\nu(O_{Ba})$, respectively.

One more criterion for classifying vibrations as intra- or interlayer vibrations may be the amplitude of the dispersion of the respective branch. It can be seen from Fig. 3, which presents calculated and experimentally measured dispersion curves, that the optical vibrations may be divided into two kinds, which differ with respect to the behavior of the dispersion branch in the $\Gamma \rightarrow Z$ direction. The high-frequency optical vibrations exhibit virtually no dispersion (attesting to the negligibly small role of the interlayer interactions in this case), while, the low-frequency branches are characterized by appreciable dispersion.

The kinds of vibrational branches obtained by inelastic neutron scattering for different perovskite-like compounds, viz., $YBa_2Cu_3O_7$ (Fig. 3) (Ref. 31), La_2CuO_4 (Ref. 32), and Nd_2CuO_4 (Ref. 33), confirm the existence of two types of behavior for these branches in the $\Gamma \rightarrow Z$ direction: the low-frequency vibrations have appreciable dispersion, while the high-frequency vibrations have virtually no dispersion.

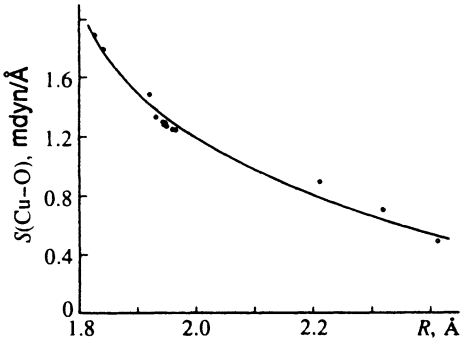

FIG. 2. Dependence of the force constant S(Cu–O) on the interatomic distance R(Cu–O).

4. VIBRATIONS OF ISOLATED LAYERS

To calculate the vibrational spectra of isolated layers in the $YBa_2Cu_3O_7$ crystal lattice, all the force constants describing interlayer interactions were set equal to zero (see the column labeled "layers" in Table I). The results obtained with the use of such a force field are presented in Table II (in the column labeled "layers"). It can be seen from the table that the frequencies of the vibrations which were classified as interlayer modes as a result of the foregoing analysis vanish, confirming the correctness of the present approach.

In addition, the frequencies of the intralayer vibrations of the O_{Cu1} atoms along the oxygen chains parallel to the x axis (B_{3u} symmetry) and to the z axis (B_{1u} symmetry) vanish. At the same time, the frequency of the vibration of the

TABLE IV. Experimental and calculated values of the elastic constants C_{ik} (GPa) in compounds with a 123 structure.

Compound	C_{11}	C_{22}	C_{33}	C_{44}	C_{55}	C_{66}	C_{12}	C_{13}	C_{23}	
$YBa_2Cu_3O_7$	211	-	159	-	-	-	-	-	-	Experiment[45,46]
$YBa_2Cu_3O_7$	207	-	63	31,36	-	85	-	-	-	Experiment[47]
$YBa_2Cu_3O_7$	230	-	150	50	-	85	100	100	-	Experiment[48]
$YBa_2Cu_3O_7$	-	244	-	61	47	97	37	89	93	Calculation[49]
$YBa_2Cu_3O_7$	315	275	279	-	-	-	-	-	-	Calculation[50]
$YBa_2Cu_3O_7$	181	235	167	50	47	59	50	94	82	Calculation[a]
$YBa_2Cu_3O_6$	176	176	140	41	41	57	45	77	77	Calculation[a]
$GdBa_2Cu_3O_7$	178	236	167	48	43	60	51	95	77	Calculation[a]

[a]Results of the present work.

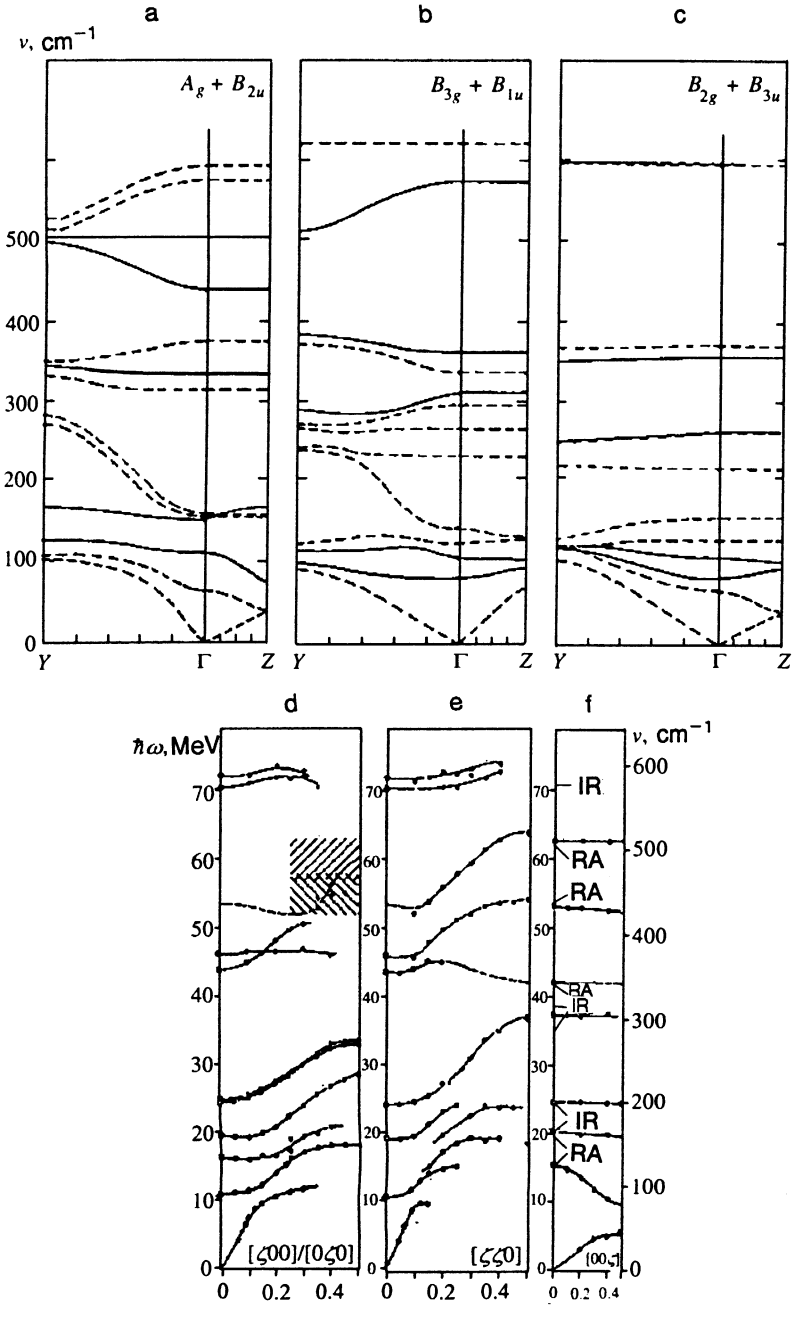

FIG. 3. Dispersion of the vibrational branches in $YBa_2Cu_3O_7$ crystals: a–c) calculated values (the solid curves correspond to vibrations which are even at the center of the Brillouin zone, and the dashed lines correspond to vibrations which are odd at the center of the Brillouin zone); d–f) experimental data.[31]

O_{Cu1} atoms along a chain parallel to the y axis (588 cm^{-1}) scarcely differs from the frequency of the corresponding vibration in the bulk crystal (593 cm^{-1}). Therefore, the $-O_{Cu1}-Cu1-O_{Cu1}-Cu1-$ chains of atoms cannot be treated as a separate layer in the force field model under discussion.

When the remaining intralayer vibrations are considered, two cases should be distinguished. The frequencies of the intralayer vibrations of the atoms along the z axis, i.e., in the direction perpendicular to the plane of the layers (A_g and B_{1u} symmetry), differed very significantly from the frequencies of the corresponding vibrations in the crystal. Therefore, the influence of the neighboring layers on such vibrations is fairly great. At the same time, the frequencies of most of the vibrations of atoms in the planes of the layers (B_{2g}, B_{3g}, B_{2u}, and B_{3u}) varied only slightly, confirming the physical plausibility of their description as layer modes.

5. QUASI-TWO-DIMENSIONAL BEHAVIOR OF THE PHONON SUBSYSTEM OF PEROVSKITE-LIKE SUPERCONDUCTORS

It was concluded in Refs. 34 and 35 that the phonon subsystem in Bi-containing superconductors exhibits quasi-two-dimensional behavior. This conclusion was based, in particular, on the results of comparing the frequencies of the Raman-active vibrations in the spectra of compounds formed as a result of the successive addition of new layers in a specially selected series of bismuth structures: $(Bi,Ca)O_\delta \rightarrow (Bi,Sr)O_\delta \rightarrow Bi_2Sr_2CuO_6 \rightarrow Bi_2Sr_2CaCu_2O_8 \rightarrow Bi_2Sr_2Ca_2Cu_3O_{10} \rightarrow Bi_4Sr_4CaCu_3O_{14}$. The high-frequency lines shift only slightly in the transition from one compound to another; therefore, it may be assumed that they are determined predominantly by intralayer interatomic forces.

The same behavior of the high-frequency Raman-active vibrations upon variation of the set of layers is also observed for two known families of thallium superconductors: $TlBa_2Ca_{n-1}Cu_nO_{2n+3}$ and $Tl_2Ba_2Ca_{n-1}Cu_nO_{2n+4}$, where $n=1,2,3$ (Refs. 36 and 37). It is important to stress that this behavior is accompanied by appreciable shifts of the low-frequency lines, which, by analogy with the interpretation discussed for 123 compounds, should be associated with vibrations of the layers relative to one another. This behavior of the low-frequency vibrations was not explained in Ref. 37, where the "traditional" one-vibration-one-type-of-atom interpretation of Raman spectra was employed, since the variations in the frequencies did not correlate with the variations in the lengths of the corresponding interatomic distances. Under the approach considered in the present work, the significant variation of the frequencies of the interlayer modes when the set of layers varies is perfectly natural.

Thus, our analysis of the vibrational spectra of three classes of compounds, viz., 123 compounds, bismuth compounds, and thallium compounds, leads to the conclusion that the dynamic properties of the crystal lattices are determined by the layered nature of these structures and that the phonon subsystem of perovskite-like superconductors has a quasi-two-dimensional character. *Two types of optical vibrations, viz., interlayer and intralayer vibrations, can be identified in the spectra of these compounds (Fig. 4).* The interlayer optical vibrations are characterized mainly by displacement of the layers as a whole relative to one another

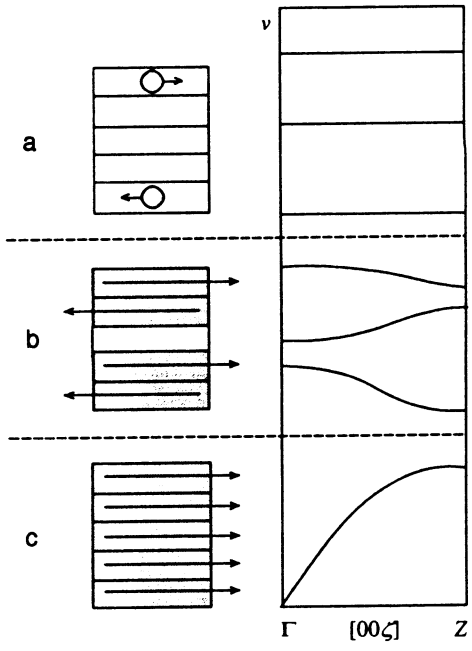

FIG. 4. Schematic representation of three different types of vibrations in the layered structure of $YBa_2Cu_3O_7$ and their dispersion in the $\Gamma \rightarrow Z$ direction: a) intralayer optical vibrations; b) interlayer optical vibrations; c) acoustic vibrations.

and have low frequencies and considerable dispersion in all directions of the Brillouin zone, including the $\Gamma \rightarrow Z$ direction. The intralayer optical vibrations occupy the high-frequency region of the spectrum, are confined mainly to displacements of the oxygen atoms, and "are localized" in layers of identical composition. If these layers are separated in the structure by several layers of another composition, the interlayer interaction is weak and there is no dispersion of the intralayer vibrations in the $\Gamma \rightarrow Z$ direction.

6. WAVE-LIKE RESTRUCTURING OF THE CRYSTAL LATTICE OF A 123 COMPOUND

The anisotropic character of the crystal lattice of a 123 compound is also manifested by its behavior when the composition is varied. In Ref. 18 such restructuring was called wave-like, if variation of the composition is accompanied by increases in some interatomic atomic distances and simultaneous decreases in others. For example, it may be concluded from the results of the x-ray structural investigation of the $YBa_2Cu_3O_{7-\delta}$ system in Ref. 24 that variation of the oxygen content δ in a 123 compound causes just such wave-like restructuring along the z axis: when the oxygen content is increased from 6.24 to 6.97, the lattice constant c decreases by 0.117 Å, and the Cu1–Cu interatomic distance decreases by 0.081 Å, while the Y–Ba interatomic distance increases by 0.055 Å (Fig. 1b). Comparing the results obtained as a result of x-ray structural investigations of 123 compounds with Y→Gd (Ref. 25) and Y→Tm (Ref. 38) substitutions, we note that wave-like restructuring also takes place as the rare-earth element R is varied. Figure 1b schematically reflects such evolution in both cases, viz., when δ is varied and under a Y→R substitution.

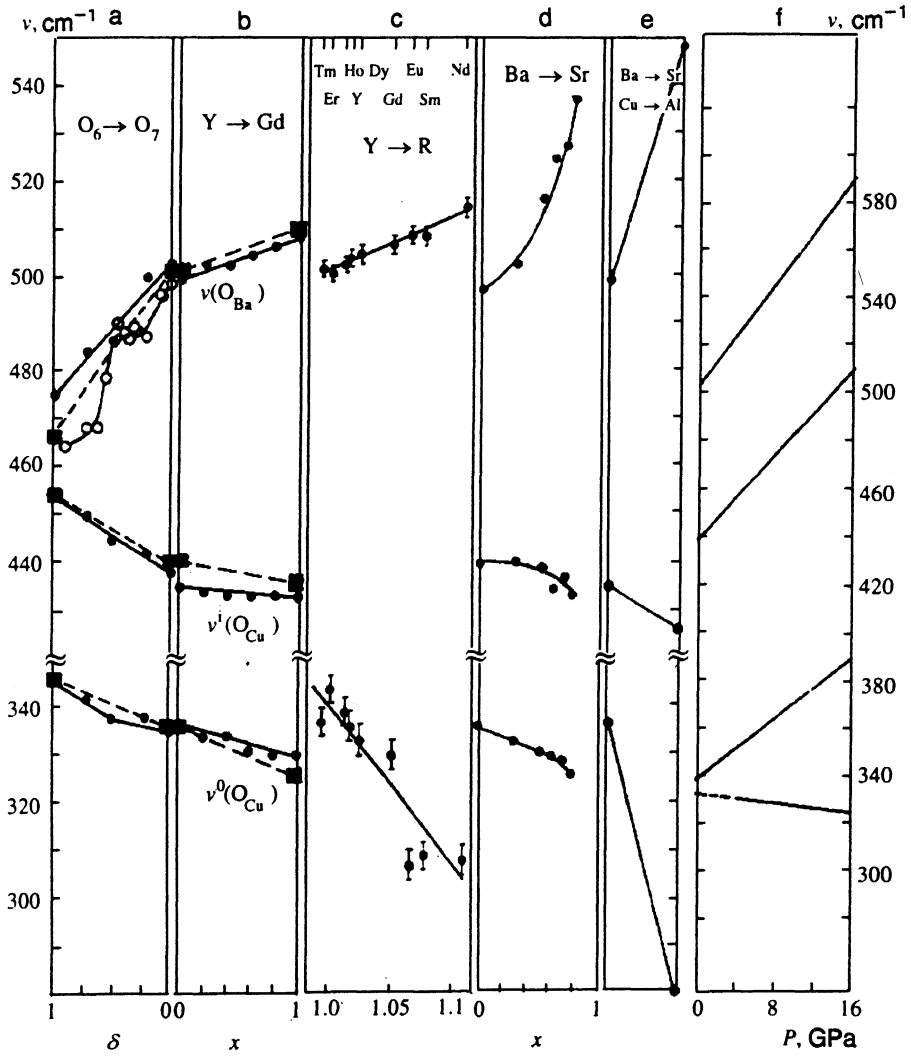

FIG. 5. Concentration-dependent behavior of the frequencies of the A_g vibrations of the oxygen atoms [$\nu^0(O_{Cu})$, $\nu^i(O_{Cu})$, and $\nu(O_{Ba})$] when the composition of $YBa_2Cu_3O_7$ is varied: a) $YBa_2Cu_3O_{7-\delta}$ according to data from Refs. 42 (filled circles) and 43 (unfilled circles); b) $(Y_{1-x}Gd_x)Ba_2Cu_3O_7$ (Ref. 16); c) dependence of $\nu^0(O_{Cu})$ and $\nu(O_{Ba})$ on the ionic radius r_i of the rare-earth element upon Y→R substitutions (Ref. 39); d) $Y(Ba_{1-x}Sr_x)_2Cu_3O_7$ (Ref. 40); e) $Y(Ba,Sr)_2(Cu,Al)_3O_7$ (Ref. 19); f) baric dependence for $YBa_2Cu_3O_7$ (Ref. 53). The squares connected by dashed lines in parts *a* and *b* are calculated results.

The changes corresponding to this effect in the vibrational spectra can be assessed by analyzing the concentration dependence of the frequencies of the A_g vibrations of oxygen atoms $\nu^0(O_{Cu})$, $\nu^i(O_{Cu})$, and $\nu(O_{Ba})$, which are observed in the Raman spectra in the form of three relatively intense lines. Since the oxygen atoms belong to different layers of the perovskite-like 123 lattice, these vibrations contain information on its modification in response to different compositions.

We previously investigated the Raman spectra of 123 compounds for different compositions: with the Y atoms replaced by Gd (Ref. 16) and by Pr (Ref. 14), with Ba replaced by Sr and Cu replaced by Al (Ref. 18), and with the oxygen content δ varying from 0 to 1 (Ref. 17). The results of these studies are presented in Fig. 5, where other published data are also given. As can be seen from the figure, when the composition is varied, the concentration-dependent shift of the lattice vibrations obeys a single law in all cases: $\nu^0(O_{Cu})$ and $\nu^i(O_{Cu})$ decrease, while $\nu(O_{Ba})$ increases.

The universality of this behavior of the vibrations is demonstrated by other experimental data known from the literature. For example, the isovalent replacement of Y^{3+} by various rare-earth elements R^{3+} with an increase in the ionic radius was accompanied by a nearly linear increase in $\nu(O_{Ba})$ and a decrease in $\nu^0(O_{Cu})$ (Fig. 5c).[39]

The influence of the isovalent replacement of Ba atoms on the vibrational frequencies was studied in Ref. 40 (Ba→Sr) and in Ref. 41 (Ba→Ca). In Ref. 40 the Raman spectra of $YBa_{2-x}Sr_xCu_3O_{7-\delta}$ were obtained for the concentrations $0 \leqslant x \leqslant 1.5$, where the solid solutions form a continuous series and have an orthorhombic structure. The results attest to the fact that as the concentration of Sr increases, $\nu^0(O_{Cu})$ and $\nu^i(O_{Cu})$ decrease, and $\nu(O_{Ba})$ increases.

Numerous investigations have been devoted to studying the influence of the oxygen content δ on the Raman spectra of $YBa_2Cu_3O_{7-\delta}$ (see, for example, Refs. 42 and 43). Despite some differences in the values of the frequencies, the results in all these studies nearly coincide qualitatively: the shifts of the $\nu^0(O_{Cu})$ and $\nu^i(O_{Cu})$ lines are opposite in sign to the shift of $\nu(O_{Ba})$ (Fig. 5a).

Thus, for very different variations of the composition, the concentration-induced changes in $\nu^0(O_{Cu})$ and $\nu^i(O_{Cu})$, on the one hand, and the concentration-induced changes in $\nu(O_{Ba})$, on the other hand, are opposed (Fig. 5). This can be explained by taking into account the forms of the vibrations (Tables II and III) and the nature of the restructuring. In fact,

as the oxygen content in $YBa_2Cu_3O_{7-\delta}$ increases, $\nu(O_{Ba})$, which corresponds to a vibration of the O_{Ba} atoms at "compression" sites in the lattice along the z axis, should increase [the bonds should shorten and become stiffer (Fig. 1)], while the frequencies $\nu^o(O_{Cu})$ and $\nu^i(O_{Cu})$ of vibrations of the O_{Cu} and O'_{Cu} atoms, which are located at "expansion" sites, should decrease (the bonds should lengthen), as is observed experimentally. On the basis of the concentration dependence of $\nu^o(O_{Cu})$, $\nu^i(O_{Cu})$, and $\nu(O_{Ba})$, it may be concluded that the nature of the wave-like restructuring is inherently related to the structure of the layers in the 123 crystal lattice, as occurs for any variations of its composition. In addition, the experimentally observed oppositely directed concentration-induced shifts of $\nu^o(O_{Cu})$ and $\nu^i(O_{Cu})$ in comparison with $\nu(O_{Ba})$ have been qualitatively explained on a single basis.

Let us take the results of these calculations and compare them with the experimental data. It is seen from Fig. 5 that in the cases considered in the present work (the Y→Gd substitution and variation of the oxygen concentration δ) the behavior of $\nu^o(O_{Cu})$, $\nu^i(O_{Cu})$, and $\nu(O_{Ba})$ obtained from the calculation fits the experimental data.

We note that the authors of most of the published calculations were unable to correctly reproduce the difference between $\nu^o(O_{Cu})$ and $\nu^i(O_{Cu})$. According to the experimental data for $YBa_2Cu_3O_7$, these frequencies are $\approx$335 and $\approx$435 cm^{-1} (the difference between them thus amounts to $\approx$100 cm^{-1}). At the same time, the calculated difference was 20 cm^{-1} in Ref. 9, 23 cm^{-1} in Ref. 6, and 316 cm^{-1} in Ref. 8, and $\nu^o(O_{Cu})$ and $\nu^i(O_{Cu})$ changed places in Ref. 7: the frequency of the antiphase vibration $\nu^o(O_{Cu})\approx 421$ cm^{-1} was higher than the frequency of the synphase vibration $\nu^i(O_{Cu})\approx 412$ cm^{-1}.

The correspondence of $\nu^o(O_{Cu})$ and $\nu^i(O_{Cu})$ to their experimental values was achieved in the present study by taking into account the dynamic interaction of the $Y-O_{Cu}$ and $Y-O'_{Cu}$ bonds (the constant H_2), i.e., by, in fact, taking into account the interaction of $CuO_{Cu}O'_{Cu}$ layers through a layer of Y atoms.

7. ELASTIC PROPERTIES OF THE CRYSTAL LATTICE OF 123 COMPOUNDS

The elastic constants C_{ik} were calculated for $YBa_2Cu_3O_7$, $YBa_2Cu_3O_6$, and $GdBa_2Cu_3O_7$ using the model under discussion. We note that the experimental data published in the literature on these very important physical characteristics are meager and often contradictory (see Ref. 44 and Table IV), largely due to the small size of the currently available single crystals of 123 compounds. The theoretical estimates of C_{ik} presented in Table IV do not make the picture more definite. At the same time, the calculations which we performed made it possible not only to determine the values of the elastic constants, but also to isolate the contributions of different interatomic interactions to the C_{ik}, as well as to analyze the influence of the anisotropy of the structure on the elastic properties.

Table IV presents the complete set of the elastic constants C_{ik} calculated on the basis of the model parameters listed in Table I. We recall that these parameters were determined by adjusting the calculated values of the vibrational frequencies without consideration of any experimental values from Table IV. Nevertheless, our results are in good agreement with the data in Refs. 45, 46, and 48, thus allowing us to regard the calculated values obtained in Ref. 50 and the experimental estimate of C_{33} given in Ref. 47 as unlikely.

According to the present work, the picture of the elastic properties of the lattice of 123 compounds is characterized by the relationship $C_{11}, C_{22} > C_{33}$, which is perfectly natural for structures having a layered structure. It should be noted that the values of C_{11} and C_{22} are only slightly greater than C_{33}.

An analysis of the dependence of C_{ik} on the force constants of the model potential function of the $YBa_2Cu_3O_7$ lattice reveals that the very stiff $Cu1-O_{Ba}$ bond does not have an appreciable influence on any of them. The elastic constant C_{11} is determined mainly by the stiffness of the $Cu-O_{Cu}$ bonds and, to a lesser extent, by the stiffness of the $Ba-O_{Ba}$ and $Ba-O'_{Cu}$ bonds; the main contribution to C_{22} is made by the $Cu1-O_{Cu1}$ and $Cu-O'_{Cu}$ bonds, as well as the $Ba-O_{Ba}$ and $Ba-O_{Cu}$ bonds. Conversely, the value of C_{33} is virtually independent of the copper–oxygen force constants and is determined by the weak, but numerous interactions of the $Ba-O_{Cu}$, $Ba-O'_{Cu}$, $Ba-O_{Cu1}$, Cu–Y, and $Cu1-Ba$ types. These interactions, together with the elasticities of the O–Cu–O bonds, determine the values of C_{44}, C_{55}, and C_{66}.

According to the calculations, the contribution of the Y–O bonds to the elastic properties of the lattice of 123 compounds is determined to a greater extent by the off-diagonal Y–O/Y–O interactions through a central Y atom than by the stiffness of the Y–O "springs" themselves.

8. CRYSTAL LATTICE OF 123 COMPOUNDS UNDER HYDROSTATIC COMPRESSION

The experimental measurement of the interatomic distances in a 123 compound under hydrostatic pressure in Ref. 51 demonstrated that the compressibilities of its various fragments differ significantly. For example, in the case of $YBa_2Cu_3O_{6.60}$, the distance between the $CuO_{Cu}O'_{Cu}$ planes scarcely varies under hydrostatic compression (in the 0–0.6 GPa range investigated), but the decrease in the $Cu-O_{Ba}$ bond length is twice as fast as the mean for the z axis. In the case of $YBa_2Cu_3O_{6.93}$, although some decrease in the distance between the $CuO_{Cu}O'_{Cu}$ layers was detected, it was significantly smaller than the mean for the z axis. These results suggest that the structural relaxation of the 123 lattice under pressure is distinctly nonuniform along the z axis and is reminiscent of the above wave-like restructuring occurring in response to variation of the composition.

Note that similar behavior of the lattice parameters has also been observed in other high-T_c superconductors: in $La_{1.85}Sr_{0.15}CuO_4$ and in $Tl_2Ba_2CuO_{6+x}$ (Ref. 52) the compressibility of the analogous Cu–O bond was also significantly higher than the mean value for the z axis.

The baric dependence of the frequencies of the A_g vibrations in the Raman spectra of 123 compounds has been investigated in several studies.[53,54] Figure 5 presents plots of $\nu(P)$ borrowed from Ref. 53. The frequencies of the fundamental vibrations increase with the pressure, the Grüneisen parameters being equal to 1.6 for $\nu^o(O_{Cu})$, 1.7 for $\nu^i(O_{Cu})$,

and 1.9 for $\nu(O_{Ba})$. At the same time, the additional line which splits off from $\nu^o(O_{Cu})$ as the pressure increases (its origin was not unequivocally established by Syassen *et al.*[53]) exhibits a negative baric dependence with a parameter equal to 0.3. This finding is not unexpected in light of the wavelike restructuring discussed above.

Let us briefly dwell on the results of a calculation of the changes in the interatomic distances in a 123 lattice under hydrostatic pressure, which faithfully reproduce the experimentally observed anisotropy of the compression. The calculation method was previously described in Ref. 55. According to the calculations, along with the "usual" behavior of the lattice under hydrostatic pressure, i.e., the decreases in most of the interatomic distances, there is an "anomalous" increase in the distance along the z axis between oxygen atoms from $CuO_{Cu}O'_{Cu}$ layers separated by a layer of Y atoms (i.e., the O_{Cu}–O_{Cu} and O'_{Cu}–O'_{Cu} distances). Note that, as in the experiment, the anisotropy is displayed more strongly in $YBa_2Cu_3O_6$ and than $YBa_2Cu_3O_7$. For example, the derivatives of the corresponding bond lengths with respect to the pressure have the values

$$\frac{d(O_{Cu}-O_{Cu})}{dP}=+0.0007 \text{ Å/kbar},$$

$$\frac{d(O'_{Cu}-O'_{Cu})}{dP}=+0.0030 \text{ Å/kbar}$$

in $YBa_2Cu_3O_7$ and

$$\frac{d(O_{Cu}-O_{Cu})}{dP}=+0.0035 \text{ Å/kbar}$$

in $YBa_2Cu_3O_6$. This effect originates in the model from the coefficient H_2, whose value, as we have already mentioned, determines the difference between $\nu^o(O_{Cu})$ and $\nu^i(O_{Cu})$.

For comparison we point out that the variation of the Cu–O_{Ba} bond length is characterized by the value

$$\frac{d(Cu-O_{Ba})}{dP}=-0.0095 \text{ Å/kbar}.$$

9. CONCLUSIONS

Thus, the elastic properties, vibrational spectra, and several important features of the behavior of the 123 crystal lattice have been successfully described using the proposed model. It has been shown that the optical vibrations can be separated into interlayer and intralayer vibrations. It has been concluded that the phonon subsystem in perovskite-like superconductors has quasi-two-dimensional behavior.

It has been established on the basis of an analysis of the calculated and experimental data that the layered structure of the 123 lattice is directly reflected in some properties of the phonon subsystem, viz., the concentration dependence of the frequencies, the normal modes of vibration, and the behavior of the dispersion branches, and that the anisotropy of the dispersion of the phonon branches increases as their frequency increases.

In fact, the acoustic modes in these compounds are not strongly anisotropic: the elastic constants C_{11} and C_{22} are only slightly greater than C_{33}. The interlayer optical vibrations, which have low frequencies ($\nu<200$ cm^{-1}) and correspond to displacement of the layers as whole units relative to one another, are likewise not strongly anisotropic: they generally have appreciable dispersion along all directions of the Brillouin zone.

Unlike the acoustic and interlayer optical vibrations, the intralayer optical vibrations are characterized by pronounced anisotropy: none exhibit dispersion in the $\Gamma\rightarrow Z$ direction, but most of them have significant dispersion in directions coinciding with the plane parallel to the layers (the xy plane). The intralayer vibrations are "localized" on oxygen atoms belonging to the same layer and form the high-frequency portion of the phonon spectrum.

We thank M. B. Smirnov for assisting in the performance of the dynamic calculations, as well as Yu. É. Kitaev, A. G. Panfilov and R. A. Évarestov for some fruitful conversations and critical remarks.

This research was performed as part of the Elfon Project (No. 91084) of the State High-T_c Superconductivity Program.

[1] R. M. Macfarlane, H. Rosen, and H. Seki, Solid State Commun. **63**, 831 (1987).
[2] M. Cardona, R. Liu, C. Thomsen *et al.*, Solid State Commun. **65**, 71 (1988).
[3] C. Thomsen, M. Cardona, B. Friedl *et al.*, Solid State Commun. **75**, 219 (1990).
[4] Yu. É. Kitaev, M. F. Limonov, A. P. Mirgorodskiĭ *et al.*, Fiz. Tverd. Tela (Leningrad) **36**, 865 (1994) [Phys. Solid State **36**, 475 (1994)].
[5] F. E. Bates and J. E. Eldridge, Solid State Commun. **64**, 1435 (1987).
[6] W. Kress, U. Schröder, J. Prade *et al.*, Phys. Rev. B **38**, 2906 (1988).
[7] H. C. Gupta, Physica C **152**, 456 (1988).
[8] S. L. Chaplot, Phys. Rev. B **37**, 7435 (1988).
[9] F. E. Bates, Phys. Rev. B **39**, 322 (1989).
[10] M. V. Belousov, I. V. Ignat'ev, N. V. Orekhova, and V. Yu. Davydov, Fiz. Tverd. Tela (Leningrad) **34**, 2804 (1992) [Sov. Phys. Solid State **34**, 1500 (1992)].
[11] R. Feile, Physica C **159**, 1 (1989).
[12] *Proceedings of the International Conference on Materials and Mechanisms of Superconductivity*, High Temperature Superconductors III, Kanazawa, Japan, 22–26 July 1991, Physica C **185–189** (1991).
[13] A. A. Bush, I. S. Dubenko, M. F. Limonov *et al.*, Pis'ma Zh. Eksp. Teor. Fiz. **50**, 250 (1989) [JETP Lett. **50**, 279 (1989)].
[14] A. A. Bush, S. A. Ivanov, V. E. Zavodnik *et al.*, Sverkhprovodimost: Fiz., Khim., Tekh. **3**, 819 (1990) [Supercond., Phys. Chem. Technol. **3**, 769 (1990)].
[15] M. F. Limonov, Ju. F. Markov, A. G. Panfilov *et al.*, Solid State Commun. **75**, 511 (1990).
[16] I. N. Goncharuk, M. F. Limonov, Yu. F. Markov *et al.*, Fiz. Tverd. Tela (Leningrad) **33**, 1282 (1991) [Sov. Phys. Solid State **33**, 726 (1991)].
[17] I. N. Goncharuk, M. F. Limonov, Yu. F. Markov *et al.*, Sverkhprovodimost: Fiz., Khim., Tekh. **4**, 1741 (1991) [Supercond., Phys. Chem. Technol. **4**, 1646 (1991)].
[18] M. F. Limonov, Yu. F. Markov, A. G. Panilov *et al.*, Physica C **191**, 255 (1992).
[19] R. A. Evarestov, Yu. E. Kitaev, M. F. Limonov, and A. G. Panfilov, Phys. Status Solidi B **179**, 249 (1993).
[20] M. Born and Kun Huang, *Dynamical Theory of Crystal Lattices*, Clarendon Press, Oxford (1954) (Russ. transl. Inostrannaya Literatura, Moscow, 1958).
[21] M. B. Smirnov, Opt. Spektrosk. **65**, 311 (1988) [Opt. Spectrosc. (USSR) **65**, 186 (1988)].
[22] A. P. Mirgorodsky, M. I. Baraton, and P. Quintard, Phys. Rev. B **48**, 13326 (1993).
[23] *Dynamic Theory and Physical Properties of Crystals*, edited by A. N. Lazarev [in Russian], Nauka, St. Petersburg (1992).
[24] V. N. Molchanov, L. A. Muradyan, and V. I. Simonov, Pis'ma Zh. Eksp. Teor. Fiz. **49**, 222 (1989) [JETP Lett. **49**, 257 (1989)].

[25] A. A. R. Fernandes, J. Santamaria, S. L. Bud'ko *et al.*, Phys. Rev. B **44**, 7601 (1991).
[26] V. D. Kulakovskiĭ, O. V. Misochko, and V. B. Timofeev, Fiz. Tverd. Tela (Leningrad) **31**, 220 (1989) [Sov. Phys. Solid State **31**, 1598 (1989)].
[27] C. Thomsen, M. Cardona, W. Kress *et al.*, Solid State Commun. **65**, 1139 (1988).
[28] A. V. Bazhenov, Zh. Eksp. Teor. Fiz. **102**, 1040 (1992) [Sov. Phys. JETP **75**, 566 (1992)].
[29] A. V. Bazhenov and V. B. Timofeev, Sverkhprovodimost: Fiz., Khim., Tekh. **3**, 1174 (1990) [Supercond., Phys. Chem. Technol. **3**, S27 (1990)].
[30] C. Thomsen, in *Light Scattering in Solids VI*, edited by M. Cardona and G. Guntherodt, Springer, Berlin (1991), p. 285.
[31] W. Reichardt, N. Pyka, L. Pintschovius *et al.*, Physica C **162–164**, 464 (1989).
[32] H. Rietschel, L. Pintschovius, and W. Reichardt, Physica C **162–164**, 1705 (1989).
[33] L. Pintschovius, N. Pyka, W. Reichardt *et al.*, Physica C **185–189**, 156 (1991).
[34] A. A. Bush, Yu. E. Kitaev, M. F. Limonov *et al.*, Physica C **190**, 477 (1992).
[35] A. A. Bush, I. N. Goncharuk, Yu. É. Kitaev *et al.*, Zh. Eksp. Teor. Fiz. **102**, 1587 (1992) [Sov. Phys. JETP **75**, 857 (1992)].
[36] K. F. McCarty, B. Morosin, D. S. Ginley, and D. R. Boehme, Physica C **157**, 135 (1989).
[37] L. V. Gasparov, V. D. Kulakovskiĭ, O. V. Misochko *et al.*, Zh. Eksp. Teor. Fiz. **96**, 2115 (1989) [Sov. Phys. JETP **69**, 1196 (1989)].
[38] V. I. Voronova, V. K. Yanovskiĭ, V. N. Molchnov *et al.*, Pis'ma Zh. Eksp. Teor. Fiz. **52**, 854 (1990) [JETP Lett. **52**, 224 (1990)].
[39] M. Cardona, R. Liu, C. Thomsen, *et al.*, Solid State Commun. **65**, 71 (1988).
[40] B. A. Kolesov, N. I. Alferova, and Yu. I. Vesnin, Sverkhprovodimost: Fiz., Khim., Tekh. **5**, 314 (1992) [Supercond., Phys. Chem. Technol. **5**, 310 (1992)].
[41] G. Leising, O. Leitner, P. Kranebitter *et al.*, Physica C **153–155**, 886 (1988).
[42] C. Thomsen, R. Liu, M. Bauer *et al.*, Solid State Commun. **65**, 55 (1988).
[43] A. F. Goncharov, V. N. Denisov, I. P. Zibrov *et al.*, Pis'ma Zh. Eksp. Teor. Fiz. **48**, 453 (1988) [JETP Lett. **48**, 497 (1988)].
[44] J. Dominec, Supercond. Sci. Technol. **6**, 153 (1993).
[45] P. Baumgart, S. Blumenröder, A. Erle *et al.*, Solid State Commun. **69**, 1135 (1989).
[46] P. Baumgart, S. Blumenröder, A. Erle *et al.*, Physica C **162–164**, 1073 (1989).
[47] T. J. Kim, J. Kowalewski, W. Assmus, and W. Grill, Z. Phys. B: Condens. Matter **78**, 207 (1990).
[48] W. Reichardt, L. Pintschovius, B. Hennion, and F. Collin, Supercond. Sci. Technol. **1**, 173 (1988).
[49] H. Ledbetter and Ming Lei, J. Mater. Res. **6**, 2253 (1991).
[50] H. C. Gupta, Mod. Phys. Lett. B **2**, 811 (1988).
[51] J. D. Jorgensen, S. Pei, P. Lightfoot *et al.*, Physica C **171**, 93 (1990).
[52] H. Takahashi, J. D. Jorgensen, B. A. Hunter *et al.*, Physica C **191**, 248 (1992).
[53] K. Syassen, M. Hanfland, K. Strössner *et al.*, Physica C **153–155**, 264 (1988).
[54] V. D. Kulakovskiĭ, O. V. Misochko, V. B. Timofeev *et al.*, Pis'ma Zh. Eksp. Teor. Fiz. **47**, 536 (1988) [JETP Lett. **47**, 626 (1988)].
[55] M. B. Smirnov and A. P. Mirgorodsky, Solid State Commun. **70**, 915 (1989).

Translated by P. Shelnitz